

## In Situ Extension as an Approach for Identifying Novel $\alpha$ -Amylase Inhibitors\*

Received for publication, June 17, 2004, and in revised form, August 9, 2004  
Published, JBC Papers in Press, August 10, 2004, DOI 10.1074/jbc.M406804200

Shin Numao<sup>‡§</sup>, Iben Damager<sup>¶||</sup>, Chunmin Li<sup>¶\*\*</sup>, Tanja M. Wrodnigg<sup>‡ ‡‡</sup>, Anjuman Begum<sup>\*\*</sup>,  
Christopher M. Overall<sup>\*\*§§</sup>, Gary D. Brayer<sup>\*\*</sup>, and Stephen G. Withers<sup>‡\*\*¶||</sup>

From the <sup>‡</sup>Department of Chemistry, University of British Columbia, Vancouver, British Columbia V6T 1Z1, Canada and the Departments of <sup>\*\*</sup>Biochemistry and Molecular Biology and <sup>§§</sup>Oral Biological and Medical Sciences, University of British Columbia, Vancouver, British Columbia V6T 1Z3, Canada

**A new approach for the discovery and subsequent structural elucidation of oligosaccharide-based inhibitors of  $\alpha$ -amylases based upon autoglucosylation of known  $\alpha$ -glucosidase inhibitors is presented. This concept, highly analogous to what is hypothesized to occur with acarbose, is demonstrated with the known  $\alpha$ -glucosidase inhibitor, D-gluconohydroximino-1,5-lactam. This was transformed from an inhibitor of human pancreatic  $\alpha$ -amylase with a  $K_i$  value of 18 mM to a trisaccharide analogue with a  $K_i$  value of 25  $\mu$ M. The three-dimensional structure of this complex was determined by x-ray crystallography and represents the first such structure determined with this class of inhibitors in any  $\alpha$ -glycosidase. This approach to the discovery and structural analysis of amylase inhibitors should be generally applicable to other endoglycosidases and readily adaptable to a high throughput format.**

$\alpha$ -Amylases (EC 3.2.1.1) are endoglycosidases that hydrolyze  $\alpha(1,4)$  glucosidic linkages with net retention of configuration at the anomeric center. From their primary structures, these enzymes have been classified into glycosyl hydrolase family 13 (1–3), a family that also includes  $\alpha$ -glucosidases and cyclodextrin glucanotransferases. Analysis of tertiary structures reveals that the catalytic domain of family 13 enzymes, especially the active site, is very well conserved (4–10). Indeed, a number of studies have shown that members of this family of glycosidases utilize a common double displacement catalytic mechanism (9, 11–13), in which a glycosyl-enzyme intermediate is formed and hydrolyzed with acid/base catalysis via oxocarbenium ion-like transition states (14–16).

\* This work was supported by the Canadian Institutes of Health Research. The costs of publication of this article were defrayed in part by the payment of page charges. This article must therefore be hereby marked "advertisement" in accordance with 18 U.S.C. Section 1734 solely to indicate this fact.

§ Recipient of a Canadian Institutes of Health Research Studentship. Present address: Institut für Mikrobiologie, ETH Zürich, CH-8092 Zürich, Switzerland.

¶ These authors contributed equally to this work.

|| Supported by Carlsbergfondet in Denmark.

‡‡ Supported by Erwin Schrödinger Post Doctoral Stipend J2092 by the Austrian Fonds zur Förderung der wissenschaftlichen Forschung. Present address: Institut für Organische Chemie der Technischen Universität Graz, Stremayrgasse 16, S-8010 Graz, Austria.

¶¶ To whom correspondence should be addressed: Dept. of Chemistry, University of British Columbia, 2036 Main Mall, Vancouver, BC V6T 1Z1, Canada. Tel.: 604-822-3402; Fax: 604-822-8869; E-mail: withers@chem.ubc.ca.

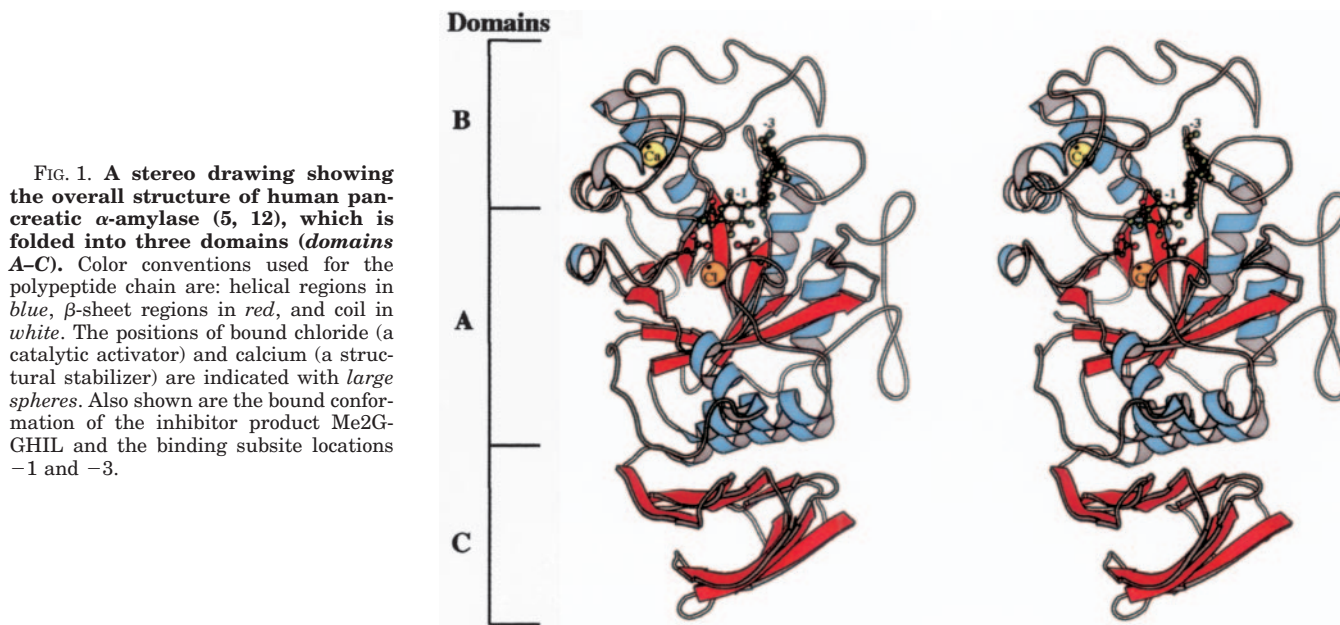
In humans, the pancreatic  $\alpha$ -amylase (HPA)<sup>1</sup> is responsible for cleaving large malto-oligosaccharides to smaller oligosaccharides, which are then substrates for intestinal  $\alpha$ -glucosidases (Fig. 1). This digestion process is important for glucose absorption from the intestine to the blood, and in principle, control of HPA activity can be used as a means of controlling blood glucose levels. In fact, HPA activity has been correlated to post-prandial blood glucose levels (17–19), and inhibitors of  $\alpha$ -amylase have been successfully used in the treatment of diseases such as diabetes or obesity where control of the blood glucose level is essential (20).

Arguably, the most studied inhibitor of  $\alpha$ -amylase is the naturally occurring and commercially available drug, acarbose (Fig. 2a), which has a  $K_i$  value in the low nanomolar range. This pseudo-tetrasaccharide is composed of a valienamine (unsaturated cyclitol) linked " $\alpha(1,4)$ " by an amine linkage to 6'-deoxy-maltotriose. The valienamine portion mimics the flattened sugar ring of the oxocarbenium ion-like transition state, whereas the exocyclic nitrogen places a proton acceptor in a position to interact with the acid/base catalyst at the active site. Indeed, with another family 13 enzyme, the CGTase from *Bacillus circulans*, this compound has been demonstrated to be a transition state analogue (21). As would be expected, structural studies of acarbose bound to HPA and other family 13 glycosidases have shown the valienamine moiety binding to the -1 subsite (22), where sugar distortion takes place in the presumed catalytic mechanism.

Interestingly, when acarbose is bound to HPA in this structure, it is modified by the enzyme through the addition of a maltosyl unit to the nonreducing end of the valienamine ring and the loss of a glucose moiety at the reducing end (Fig. 2a). The inhibitor therefore occupies all five subsites of HPA (-3 to +2). Similar, although not identical, modifications have also been seen in structural studies of other  $\alpha$ -amylases in complexes with acarbose (6, 23, 24). Because increased subsite occupancy is often associated with an increase in the overall binding affinity of an inhibitor, such a modification presumably results in a tighter binding molecule. To date, however, beyond the crystallographic data for the complex, there has been no direct evidence for such a product being formed in solution with  $\alpha$ -amylase.

Despite the considerable interest in  $\alpha$ -amylases, there are relatively few other known inhibitors of this group of enzymes.

<sup>1</sup> The abbreviations used are: HPA, human pancreatic  $\alpha$ -amylase; CGTase, cyclodextrin glucanotransferase; CNP-G3, 2-chloro-4-nitrophenyl  $\alpha$ -maltotrioside; G3F,  $\alpha$ -maltotriosyl fluoride; G2-GHIL, maltosyl- $\alpha(1,4)$ -D-gluconohydroximino-1,5-lactam; GHIL, D-gluconohydroximino-1,5-lactam; MeG2F, 4'-O-methyl  $\alpha$ -maltosyl fluoride; MeG2-GHIL, 4'-O-methyl-maltosyl- $\alpha(1,4)$ -D-gluconohydroximino-1,5-lactam; MALDI-TOF, matrix-assisted laser desorption ionization time-of-flight.



(a)

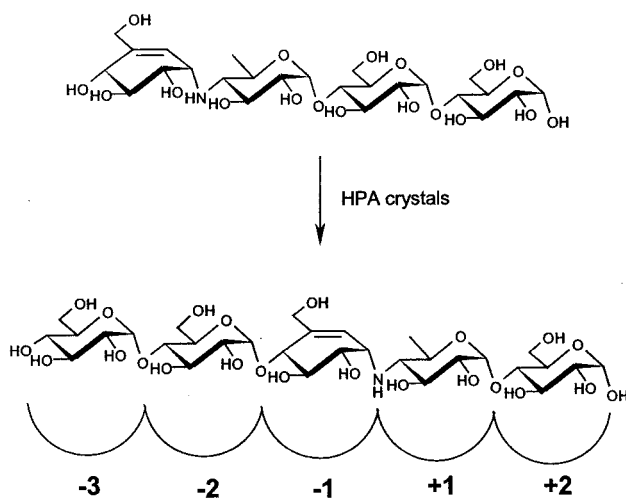
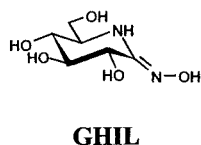


**FIG. 2. a**, structure of the  $\alpha$ -amylase inhibitor acarbose. In crystal structures of complexes with HPA, acarbose becomes modified to an extended form. The five subsites of HPA (–3 to +2) are shown as a cartoon to illustrate how the sugars bind to the respective subsites. **b**, Structure of GHIL.

(b)



From kinetic and structural studies, one would expect that the greatest transformation of the substrate on going from the ground state to the transition state will take place on the sugar occupying the –1 subsite. As such, the interactions at the –1 subsite should be particularly optimized for transition state binding, and therefore transition state mimics should bind particularly well at this site.

Because the active sites of other family 13  $\alpha$ -glucosidases are thought to be structurally similar to that of HPA, it is likely

that transition state analogues of such enzymes will interact similarly with the –1 subsite residues of  $\alpha$ -amylase. Furthermore, it seems reasonable that the affinity of the inhibitor would correlate, in part, with the number of subsites with which the compound interacts. Therefore, an  $\alpha$ -glucosidase inhibitor extended on the reducing and/or nonreducing end by a malto-oligosaccharide so as to occupy the other subsites should make a good inhibitor of  $\alpha$ -amylases. In the past, the main difficulty in testing this hypothesis has been in the synthesis of

TABLE I  
Structure determination statistics

	GHIL/HPA	GHIL/G3F/ HPA	GHIL/MeG2F/HPA
Data collection parameters			
Space group	P2 <sub>1</sub> 2 <sub>1</sub> 2 <sub>1</sub>	P2 <sub>1</sub> 2 <sub>1</sub> 2 <sub>1</sub>	P2 <sub>1</sub> 2 <sub>1</sub> 2 <sub>1</sub>
Unit cell dimensions			
<i>a</i>	52.8	52.3	52.2
<i>b</i>	68.9	68.6	67.4
<i>c</i>	132.4	131.5	130.2
No. of unique reflections	35,249	34,125	27,904
Mean <i>I</i> / $\sigma$ <sup>a</sup>	24.1 (6.3)	27.6 (11.1)	15.0 (6.4)
Multiplicity <sup>a</sup>	6.4 (3.4)	9.8 (3.3)	9.3 (2.1)
Merging <i>R</i> -factor (%) <sup>a</sup>	6.2 (18.5)	6.2 (18.0)	4.8 (19.0)
Maximum resolution (Å)	1.95	1.90	1.95
Structure refinement values			
No. of reflections	35155	33966	27842
Resolution range (Å)	10.0–1.95	10.0–1.90	10.0–1.95
Completeness within range (%) <sup>a</sup>	98.6 (96.9)	89.9 (88.9)	81.3 (80.2)
No. of protein atoms	3946	3946	3946
No. of solvent atoms	175	161	269
Average B factors (Å <sup>2</sup> )			
Protein atoms	20.4	20.2	19.8
Solvent atoms	29.3	29.8	24.6
Final <i>R</i> -factor and <i>R</i> -free (%) <sup>b</sup>	16.7/19.8	17.5/19.5	18.3/22.7
Structural stereochemistry		Root mean square deviations	
Bonds (Å)	0.007	0.007	0.011
Angles (°)	1.3	1.3	1.4

<sup>a</sup> The values in parentheses refer to the highest resolution shell (2.02–1.95 or 1.97–1.90 Å).

<sup>b</sup> 5% of the diffraction data was kept aside for the *R*-free.

such extended  $\alpha$ -glucosidase inhibitors, although some work to this end has been carried out (25–28).

In this paper, we describe a method to extend  $\alpha$ -glucosidase inhibitors *in situ*, both in solution and within  $\alpha$ -amylase crystals, by co-addition of an activated substrate. In doing so, we have been able to show that a potent  $\alpha$ -glucosidase inhibitor, D-gluconohydroximinol-1,5-lactam (GHIL; Fig. 2b) (29), which is normally a poor HPA inhibitor, is converted into a useful inhibitor of HPA. Using this method, it should be possible to assay a wide range of known  $\alpha$ -glucosidase inhibitors using a facile kinetic screen for HPA inhibition by the elongated species and then determine the structure of the elongated species crystallographically.

## EXPERIMENTAL PROCEDURES

### Materials

All of the chemicals and buffer salts were obtained from Sigma unless otherwise specified. HPA was purified according to literature procedures (30). 2-Chloro-4-nitrophenyl  $\alpha$ -maltotrioside (CNP-G3) was a generous gift from GelTex Inc. and can be purchased from Genzyme Inc.  $\alpha$ -Maltotriosyl fluoride (G3F) (31) and GHIL (32, 33) were synthesized according to literature procedures. Syntheses of 2,4-dinitrophenyl  $\alpha$ -maltotrioside and 4'-*O*-methyl  $\alpha$ -maltoosyl fluoride (MeG2F) will be published elsewhere.

### Kinetic Analyses

**General**—All of the studies were carried out at 30 °C in 50 mM sodium phosphate buffer, pH 6.9, containing 100 mM NaCl, unless otherwise described. Hydrolysis of CNP-G3 by HPA was monitored after the addition of enzyme by following the increase in absorbance at 400 nm using a Varian CARY 4000 spectrophotometer attached to a temperature control unit. The hydrolysis of G3F by HPA was monitored by following the increase in fluoride concentration upon the addition of enzyme using an ORION 96–04 combination fluoride electrode interfaced to a personal computer running the program LoggerPro (Vernier Software, Oregon). All analyses of the data were accomplished using the program GraFit 4.0.21 (34).

**Extension Kinetics and Product Analyses**—Extension studies were accomplished by preincubating HPA with G3F (0.2 mM) and acarbose (180 nM), or G3F (0.4 mM) and GHIL (1 mM). After 1 h, the residual activity of HPA was measured by the addition of CNP-G3 and meas-

uring the increase in absorbance at 400 nm. Control reactions were done in the absence of either the G3F or inhibitor.

Product formation in the HPA-catalyzed reaction of G3F with GHIL was monitored by MALDI-TOF mass spectrometry analysis. G3F and GHIL were incubated with HPA (0.06 mg/ml) for 1 h at 30 °C in 5 mM sodium phosphate buffer, pH 6.9, containing 10 mM NaCl. A saturated solution of 2,5-dihydroxybenzoic acid in deionized water was used as the matrix. The sample and matrix solutions were mixed in a 1:20 ratio, and 1  $\mu$ l of this sample was spotted on the target plate and dried *in vacuo*. The MALDI-TOF spectra were collected using a Voyager-DE-STR (Applied Biosystems) mass spectrometer in reflectron mode with an acceleration voltage of 20 kV.

**Inhibition Kinetics**—The  $K_i$  values and mode of inhibition were determined by measuring the rate of hydrolysis of either G3F (0.1225–2.45 mM) or CNP-G3 (0.5–2.0 mM) in the presence of a varying concentration of inhibitor (4–5 points). The data were fit using the program GraFit 4.0.21 (34) and plotted in the form of a Dixon plot (1/rate versus [inhibitor]) to allow visual inspection of the data.

### Synthesis of Elongation Product

Enzymatic coupling of MeG2F (1.6 mg, 4.5 mmol) and GHIL (1.0 mg, 5.2 mmol) dissolved in 25  $\mu$ l of 50 mM citrate buffer, pH 6.0, was accomplished by incubating the two compounds in the presence of CGTase (2.2  $\mu$ l, 50 ng/ml) at 30 °C for 16 h. The reaction was monitored by MALDI-TOF mass spectrometry. After completion, the reaction mixture was freeze-dried, and the residue was purified by column chromatography using a water/acetonitrile solution as eluent (v/v, 1:4) to yield pure MeG2-GHIL in 70% yield (1.7 mg). Further characterization of the product was achieved after per-*O*-acetylation using acetic anhydride in pyridine overnight. The solvent was evaporated *in vacuo*, and the residue was dissolved in EtOAc. The solution was washed with aqueous HCl (1 M), saturated aqueous NaHCO<sub>3</sub>, and brine and then dried over MgSO<sub>4</sub>. NMR data: <sup>1</sup>H NMR (CDCl<sub>3</sub>, 600 MHz):  $\delta$  5.81 (bs, 1 H, NH), 5.36 (m, 2 H, H-3, H-3'), 5.33 (m, 1 H, H-3''), 5.13 (d, 1 H, H-2), 5.06 (d, 1 H, H-1'), 4.89 (d, 1 H, H-1'), 4.78 (dd, 1 H, H-2''), 4.74 (t, 1 H, H-4), 4.56 (dd, 1 H, H-2'), 4.46 (dd, 1 H, H-6a'), 4.28 (dd, 1 H, H-6a''), 4.06 (m, 3 H, H-6b', H-5, H-6a), 3.93 (m, 2 H, H-6b, H-5'), 3.79 (dd, 1 H, H-6b''), 3.60 (t, 1 H, H-4'), 3.32 (m, 1 H, H-5'), 3.10 (s, 3 H, OCH<sub>3</sub>), 3.00 (t, 1 H, H-4'), 2.25–1.95 (10 s, 30 H, COCH<sub>3</sub>).

### Structural Determinations

Crystals of HPA were grown using conditions previously described (22). The HPA/GHIL inhibitor complex was prepared for structural

analysis by soaking a HPA crystal in a solution containing 100 mM GHIL for 24 h. A crystal of HPA complexed with both GHIL and G3F was prepared by first soaking in a solution containing 100 mM GHIL for 2 h followed by a 1-h soak in a solution containing 100 mM G3F. A similar approach was used in the formation of the complex with GHIL and MeG2F.

Diffraction data for all complex crystals were collected on a Mar345 imaging plate area detector system at 100 K using copper  $K\alpha$  radiation supplied by a Rigaku RU300 rotating anode generator operating at 50 kV and 100 mA. Intensity data were integrated, scaled, and reduced to structure factor amplitudes, with the HKL suite of programs (35). Data collection statistics are provided in Table I. The crystals of all of the complexes were isomorphous with that of HPA alone (22), and as such, this structure was used as the starting refinement model for these complexes. Refinement was carried out with the CNS software program (36). In these analyses, cycles of simulated annealing, positional, and thermal B refinements were alternated with manual model rebuilding with O (37). In the initial stages of this process, the complete polypeptide chain of the refinement model was adjusted based on a composite annealed omit map (with 3% of the residues omitted per segment). Subsequently, the complete polypeptide chain was examined periodically with  $F_o - F_c$ ,  $2F_o - F_c$  and omit difference electron density maps. Following the refinement of the polypeptide chain of HPA, bound inhibitor molecules were positioned on the basis

of  $F_o - F_c$  difference electron density maps. For both complexes, protein and inhibitor atoms were then jointly refined to obtain the best overall fit. In addition, an *N*-acetylglucosamine moiety bound to the side chain of Asn<sup>461</sup> was included in the structural model and refined accordingly. At this point, solvent molecules were identified from a further  $F_o - F_c$  difference electron density map and included in the refinement model based on the hydrogen bonding potential to protein atoms and the refinement of a thermal factor of  $<75 \text{ \AA}^2$ . In a final phase, the protein, inhibitor, and solvent molecules were jointly refined to convergence. The final refinement statistics obtained are detailed in Table I.

## RESULTS AND DISCUSSION

**Kinetic Analyses**—The concepts described herein first evolved out of our attempts to determine whether simple “monosaccharide” inhibitors of  $\alpha$ -glucosidases would also function as useful inhibitors of HPA. As our best candidate, we investigated the potent  $\alpha$ -glucosidase inhibitor GHIL ( $K_i = 2.9 \mu\text{M}$  with yeast  $\alpha$ -glucosidase (29)). The assays were initially conducted with the substrate  $\alpha$ -maltotriosyl fluoride ( $k_{\text{cat}} = 200 \text{ s}^{-1}$ ,  $K_m = 0.5 \text{ mM}$ ) using a fluoride electrode. In this way, a  $K_i$  value of 1.8 mM was obtained. Although this inhibition is too weak to be therapeutically useful, it did suggest that this, and other such monosaccharides might be valuable inhibitors by providing a starting point for the design of extended and potentially more potent inhibitors that also occupy additional sugar binding subsites in the enzyme active site. Indeed, strong indications that elongation of these inhibitors with additional glucose residues might lead to substantial increases in affinity come from two findings. First, the  $k_{\text{cat}}/K_m$  values for oligosaccharide substrates were observed to significantly increase upon the addition of glucose moieties to the nonreducing end of a substrate. This points to substantial transition state stabilization from these additional sugar residues because the  $k_{\text{cat}}/K_m$  values increase from  $98 \text{ s}^{-1} \text{ mM}^{-1}$  to  $830 \text{ s}^{-1} \text{ mM}^{-1}$  on going from maltosyl fluoride to maltotriosyl fluoride (22). Second, several studies have shown that oligosaccharide-based molecules are better inhibitors of the related porcine pancreatic  $\alpha$ -amylase (25–27).

To more easily assay  $\alpha$ -amylase inhibitors, a simple, chromogenic assay involving the commercially available substrate,

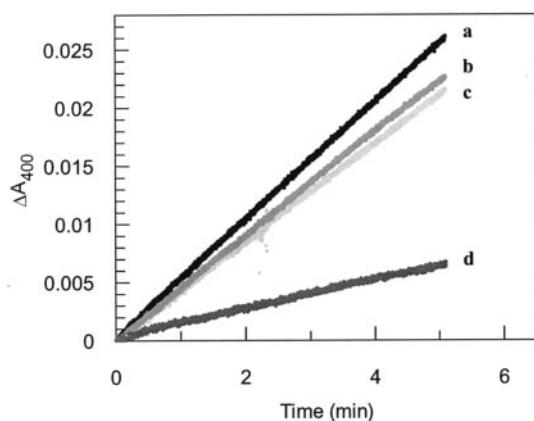


FIG. 3. CNP-G3 hydrolysis catalyzed by HPA after preincubation for 15 min with glucose (a), GHIL (b), glucose + G3F (c), and GHIL + G3F (d).

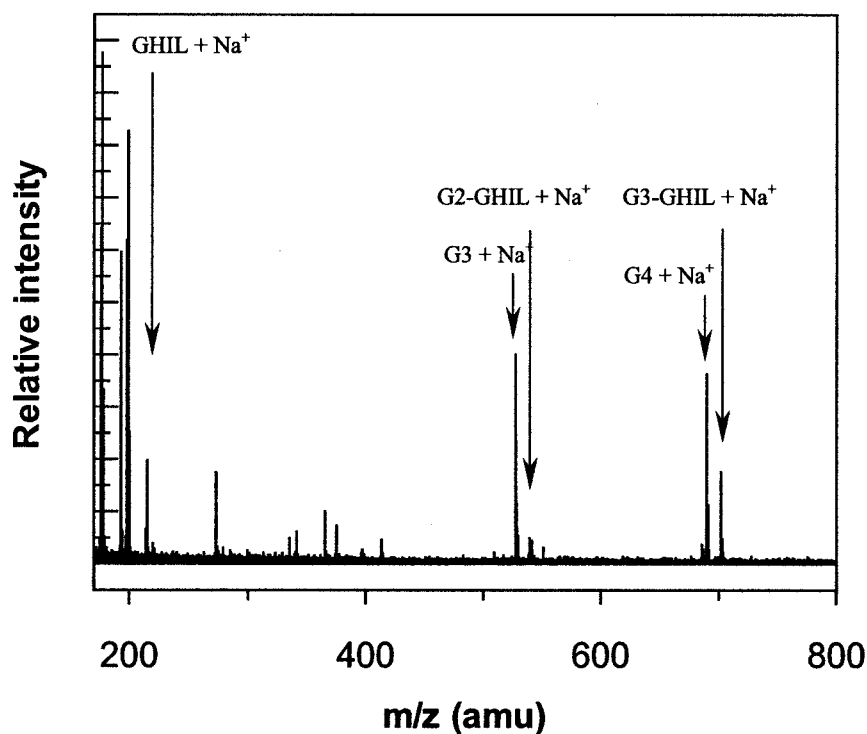
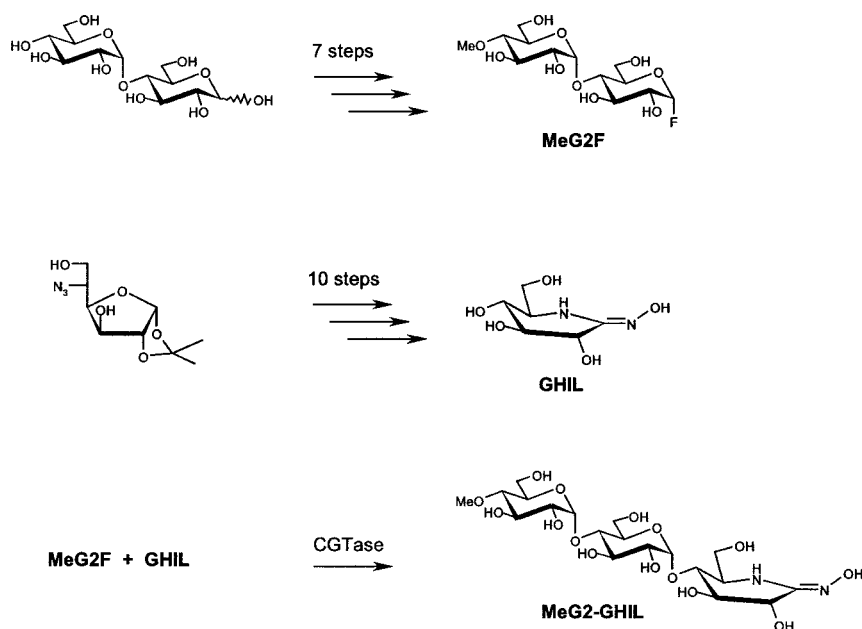


FIG. 4. Product analysis by MALDI-TOF mass spectrometry of the HPA-catalyzed reaction between G3F and GHIL.

FIG. 5. General synthetic scheme for MeG2-GHIL.



CNP-G3 ( $k_{\text{cat}} = 1.9 \text{ s}^{-1}$ ,  $K_m = 3.6 \text{ mM}$ ) was employed. To our surprise, using this compound as a substrate, a  $K_i$  value of 18 mM was found for GHIL, which is 10-fold higher than that measured using G3F as substrate. This unusual behavior merited further analysis because other data ensured that this was not an “artifact” of kinetic analysis and that there was indeed a change in the apparent affinity of HPA for GHIL depending on the substrate.

Supportive evidence for such a change in inhibitory activity is evident when assaying for HPA activity with CNP-G3 at higher concentrations of GHIL, when a time-dependent decrease in rate was observed over a period of 20 min. No such time-dependent decrease was observed in the absence of inhibitor, eliminating substrate depletion as the cause of this phenomenon. Preincubation of HPA with GHIL prior to measurement of activity with CNP-G3 did not decrease initial rates, thereby eliminating both covalent inactivation and slow on rates as possible causes of this behavior. The most likely explanation for both the difference in  $K_i$  values and the time-dependent behavior is that during the kinetic analysis of GHIL with CNP-G3, slow transglycosylation of a maltotriose moiety to GHIL is occurring. This would yield an elongated version of GHIL that binds much more tightly than the original molecule, analogous to what is presumed to occur in crystals of HPA soaked with acarbose. However, because G3F is a much better substrate for HPA than is CNP-G3 ( $k_{\text{cat}}/K_m$  value is 1800 times greater than for CNP-G3), the maltotriose moiety will likely be transglycosylated to the inhibitor at a higher rate when working with G3F compared with CNP-G3. If this were the case, the “steady state” concentration of elongated species is quickly reached and at higher levels when using G3F than when using CNP-G3, thereby accounting for the 10-fold lower  $K_i$  value determined. For the more slowly reacting CNP-G3, formation of the steady state concentration of the elongated species occurs more slowly and is seen instead as a slow decrease in the catalytic activity over time.

To probe this hypothesis further, HPA was preincubated with GHIL (0.4 mM) and G3F (1 mM) for 15 min prior to assay using CNP-G3 (1 mM). If an extended inhibitor is formed, then HPA should be inhibited under these conditions, even if the assay is done with CNP-G3. The rate determined under these conditions was  $\sim 25\%$  of the rate of a control reaction in which

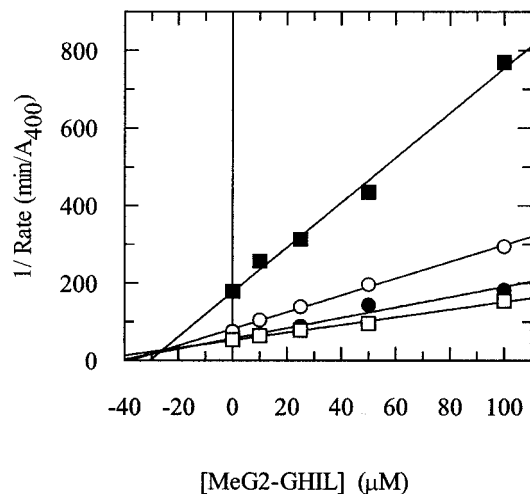


FIG. 6. Dixon plot analysis of the inhibition of HPA by MeG2-GHIL using CNP-G3 at concentrations of 0.5 mM (■), 1.0 mM (○), 2.0 mM (●), and 3.0 mM (□).

HPA was preincubated with G3F or GHIL alone, strongly suggesting that HPA is catalyzing a reaction between the inhibitor and substrate and that the product of this reaction is a better inhibitor of HPA (Fig. 3).

A preincubation experiment was also carried out with acarbose (180 nM) in place of GHIL and similar results obtained, with rates significantly dropping compared with those for the control reaction in which no acarbose was present (data not shown). Because structural studies have shown acarbose to form an elongated product in the presence of HPA, this result provides strong support for the idea that elongated inhibitors are the principal inhibitory species in the kinetic analysis using G3F. Notably, as one might expect from this hypothesis, preincubation of HPA with G3F and glucose did not result in a significant decrease in the rate of hydrolysis of the substrate (Fig. 3).

An attempt was made to quantitate the change in inhibitory activity by measuring an apparent  $K_i$  value for the elongated inhibitor species formed during preincubation. The experiments carried out involved incubation of varying concentrations of GHIL (0–0.6 mM) with a fixed concentration of G3F

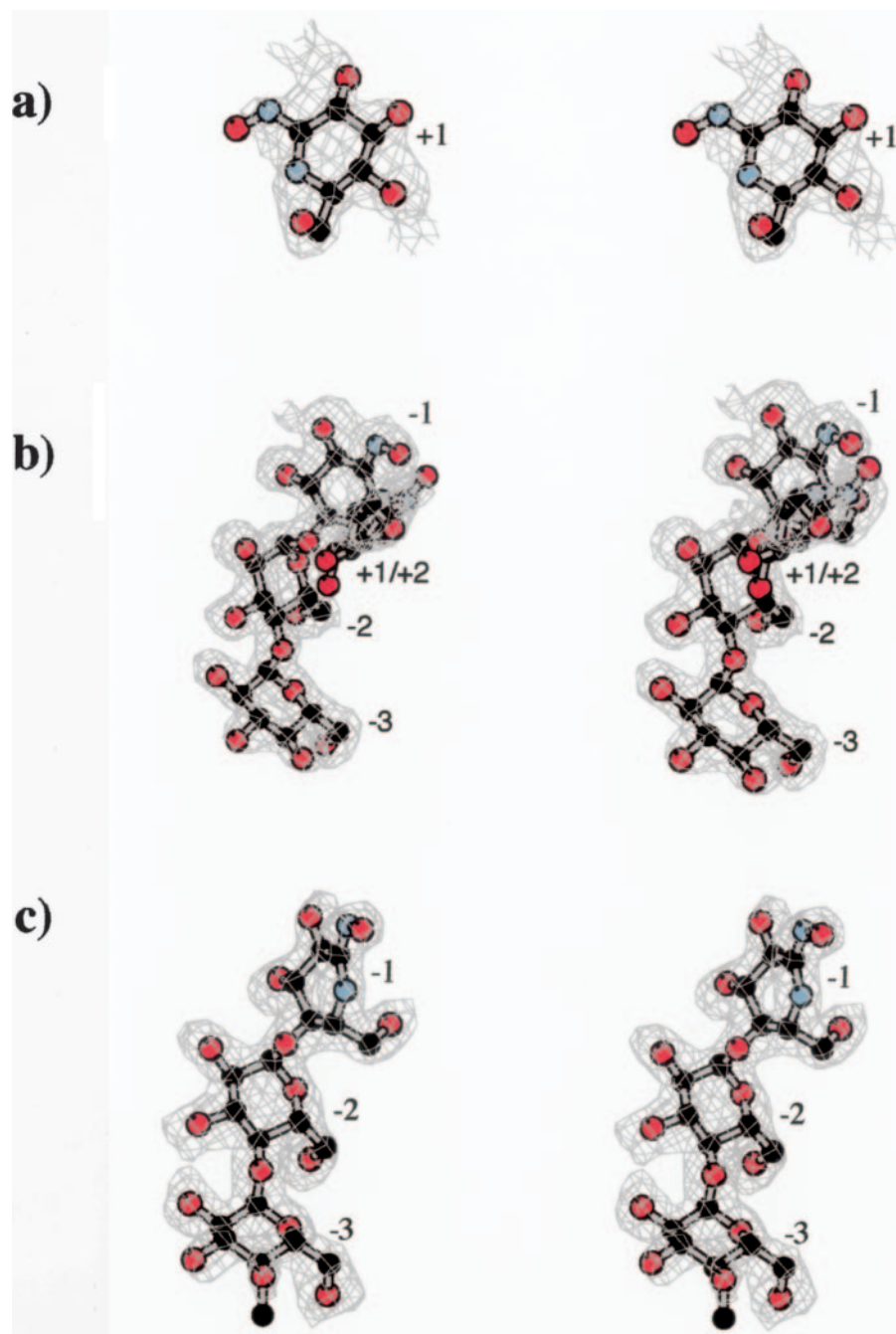


FIG. 7. Stereo plots of the omit difference electron density maps calculated for the GHIL (a), G2-GHIL and an additionally bound GHIL molecule (b), and MeG2-GHIL (c) inhibitor complexes in the active site of human pancreatic  $\alpha$ -amylase. All of the maps are drawn at the  $2\text{-}\sigma$  level and overlaid are the final refined structures of each inhibitor product. Also indicated are the positions of the binding subsites to which inhibitor atoms are bound. Atom color coding follows the convention of oxygen (red), nitrogen (blue), and carbon (black).

(0.4 mM) and HPA. After 1 h of incubation at 30 °C, the HPA activity was measured using 2,4-dinitrophenyl maltotriose (0.9 mM). Rates measured under these conditions were then plotted in the form of a Dixon plot (assuming the complete conversion of GHIL to a homogeneous inhibitory species), and an apparent  $K_i$  value of 265  $\mu\text{M}$  was extracted from the intersection between this line and the horizontal line corresponding to  $1/V_{\text{max}}$  (where  $V_{\text{max}}$  is the maximal rate of 2,4-dinitrophenyl  $\alpha$ -maltotriose hydrolysis in the presence of 0.4 mM G3F) (data not shown). In comparison with the  $K_i$  value of 18 mM determined for unmodified GHIL (no G3F preincubation), this  $K_i$  value represents an approximate 100-fold increase in affinity as a consequence of preincubation. The greater inhibition observed under these conditions than when assayed directly with G3F suggests that longer reaction times and/or higher concentrations of reactants are required to build up inhibitory concentrations, even with G3F. The  $K_i$  value de-

termined, however, represents a “worst case” estimate of the true  $K_i$  value for the inhibitor because it assumes all of the inhibitor is converted to the tight binding version, which is highly unlikely, and which mass spectrometric analysis (see below) reveals not to be the case. The true  $K_i$  value must therefore be much lower.

**Mass Spectrometric Analysis**—Initial attempts to observe an elongated GHIL species formed under the preincubation conditions discussed above by using a MALDI-TOF mass spectrometer were unsuccessful. Only products of the normal hydrolysis and transglycosylation reactions of G3F were observed, possibly because the inhibitory species is being formed at concentrations well below the sensitivity level of the instrument. Concentrations of both G3F and GHIL were therefore raised such that G3F was present at 10 times its  $K_m$  value, and GHIL was present at the  $K_i$  value of the unmodified species (18 mM). Analysis of such reaction mixtures by MALDI-TOF

mass spectrometry revealed two additional products of  $m/z$  539 and 702. These masses correspond to the sodium adducts of GHIL linked to a maltosyl or maltotriosyl moiety, respectively (Fig. 4), thereby demonstrating that HPA will catalyze the elongation of GHIL.

**Synthesis of an Extended GHIL for Further Kinetic Studies**—To demonstrate that elongated GHIL is a better inhibitor of HPA, an extended version of GHIL was synthesized using a chemo-enzymatic approach (Fig. 5). To simplify both the enzymatic synthesis and subsequent kinetic analysis of the elongated species, a “blocked” version was made in which the 4'-hydroxyl group at the nonreducing end was methylated. Such an inhibitor should not undergo further elongation at the 4"-position and therefore should remain a stable species during kinetic analysis. Synthesis of this MeG2-GHIL was achieved by incubating MeG2F overnight with GHIL in the presence of CGTase from *B. circulans*, which has been shown previously to be highly effective in transferring sugar moieties to monosaccharide analogues (27) without suffering the severe product inhibition that would be seen when using  $\alpha$ -amylases. After the initial transglycosylation, the 4'-*O*-methyl group blocks further transglycosylation reactions, resulting in a homogeneous product. This product was purified by column chromatography yielding MeG2-GHIL (1.7 mg) in 70% yield. Analysis by MALDI-TOF mass spectrometry ( $m/z = 553.2$ ; expected with sodium adduct,  $m/z = 553.4$ ) revealed the proper product formation. NMR spectra ( $^1\text{H}$  NMR, COSY, and TOCSY) of the per-*O*-acetylated derivative obtained by treating MeG2-GHIL with acetic anhydride in pyridine confirmed the  $\alpha(1,4)$  linkage formed between the maltosyl moiety and the GHIL unit.

With the pure, elongated and capped inhibitor in hand, kinetic analysis of its inhibition behavior was performed. The presence of the methyl cap should simplify kinetic analysis and allow determination of a “true”  $K_i$  value. As shown in Fig. 6, using CNP-G3 as a substrate, MeG2-GHIL was shown to be a competitive inhibitor of HPA with a  $K_i$  value of 25  $\mu\text{M}$ . This  $K_i$  value is 3 orders of magnitude lower than that for the monosaccharide inhibitor, GHIL, using CNP-G3 as a substrate, clearly demonstrating that extension of GHIL generates better inhibitors.

**Structural Analysis**—Even though GHIL has poor binding affinity for the active site of HPA, it has proven possible to determine its bound structure using crystallographic techniques (Fig. 7a). Surprisingly, this monosaccharide analogue is bound in the +1 subsite with a novel reverse ring orientation not previously observed for inhibitors bound at this subsite. This reversal of direction results in the inhibitor forming hydrogen bonding interactions (Figs. 8a and 9a) completely different from those normally observed with previously studied inhibitors such as acarbose (Fig. 9c and Ref. 22). The main interactions involve the 4-hydroxyl group with the side chain of His<sup>201</sup>, the 2-hydroxyl group with the side chain of the putative acid/base catalyst, Glu<sup>233</sup>, and a water-mediated interaction between the oxime group and the side chain of the catalytic nucleophile, Asp<sup>197</sup>. In agreement with kinetic studies, GHIL is not tightly bound in the active site of HPA, as is evident from the substantially higher thermal factors observed for atoms of this inhibitor (45.9  $\text{\AA}^2$ ) in comparison with those of the enzyme as a whole (20.4  $\text{\AA}^2$ ).

A second set of experiments in which HPA crystals were soaked with both GHIL and G3F resulted in a substantially modified inhibitor being bound in the active site of this enzyme (Figs. 8b and 9b). The species formed, presumably a product of transglycosylation and hydrolysis events catalyzed by the enzyme, is a trisaccharide analogue that spans the -3 to -1

subsites. The residue in the -1 subsite is a GHIL moiety, bound in the “normal” orientation, whereas the -2 and -3 subsites are occupied by glucosyl moieties (Figs. 8b and 9b). This maltosyl-D-gluconohydroximino-1,5-lactam (G2-GHIL) product corresponds to one of the elongated species observed by mass spectrometry (Fig. 4) and is equivalent to the MeG2-GHIL inhibitor that was synthesized and studied kinetically (Fig. 6). The electron density map for all of the G2-GHIL sugar rings is well defined, and the overall thermal B values of the individual rings are considerably lower than that observed for GHIL alone (Fig. 7b). Much weaker electron density is also seen for another separate and unmodified molecule of GHIL, bound across the +1 and +2 subsites (Fig. 9b). However, the refined thermal factors for the atoms of this group are very high, suggesting that binding in this mode is very weak.

The interactions formed by the glucose moieties of G2-GHIL in subsites -2 and -3 are very similar to the interactions observed for acarbose, as are the conformations of these sugar moieties (Figs. 8, b and c, and 9, b and c). The largest difference involves the rotation of the 6'-hydroxyl group in subsite -3, which results in this hydroxyl group interacting with a water molecule, whereas in the acarbose structure, the interaction was to Thr<sup>163</sup>. Another difference is the absence of an interaction between the 3'-hydroxyl group in subsite -2 and His<sup>305</sup> in the G2-GHIL-HPA complex.

The structure of the complex formed when HPA is soaked with MeG2F and GHIL was also determined as a comparison (Table I and Fig. 7c). Notably, the bound species has a conformation very similar to that of the G2-GHIL complex, once again demonstrating the ability of HPA to combine a poor binding inhibitor and an activated substrate to form a tight binding inhibitor. No separate, unmodified bound GHIL was observed in this case. The only significant difference between the complexes with MeG2-GHIL and G2-GHIL is the presence of the methyl group capping the 4'-hydroxyl group, showing that, with care, non-natural substitutions can be introduced into the activated substrate moiety used to transglycosylate GHIL by HPA. This provides an exciting new avenue for designing unique end products tailored to the HPA active site to maximize inhibitor binding affinity.

One of the most interesting features arising from these structural analyses is the conformation observed for the GHIL moiety of G2-GHIL and MeG2-GHIL. In solution, GHIL has been shown to adopt a  $^4\text{C}_1$  chair conformation, whereas the crystalline structure of GHIL adopts a  $^4\text{H}_3$  half-chair conformation (33). When GHIL alone is bound to HPA, it appears to adopt a  $^4\text{E}$  conformation, similar to the conformation adopted by the GHIL analogue xylobiono-lactam oxime bound to the xylanase from *Cellulomonas fimi* (38). In contrast, the GHIL moiety of G2-GHIL and MeG2-GHIL, bound to the -1 subsite of HPA, adopts an  $\text{E}_3$  conformation. A consequence of the  $\text{E}_3$  conformation is that the oxime group points toward, and is in close proximity to, the acid/base catalyst Glu<sup>233</sup>, with the exocyclic nitrogen being within hydrogen bonding distance of OE1 of the carboxylic acid group (Fig. 9b). This interaction is exactly as predicted for an anti-protonating glycosidase (39). In fact, such interactions have also been observed in the above-mentioned  $\beta$ -glycosidase, *C. fimi*  $\beta$ -xylanase, an anti-protonator from glycosidase family 10 (38, 39). In *C. fimi*  $\beta$ -xylanase, this is the only interaction between this catalytic residue and the oxime group, whereas in HPA the OE2 of Glu<sup>233</sup> is also in close proximity to the oxime hydroxyl group.

From modeling studies it can be seen that, should the GHIL moiety of the bound G2-GHIL adopt a  $^4\text{E}$  conformation as was

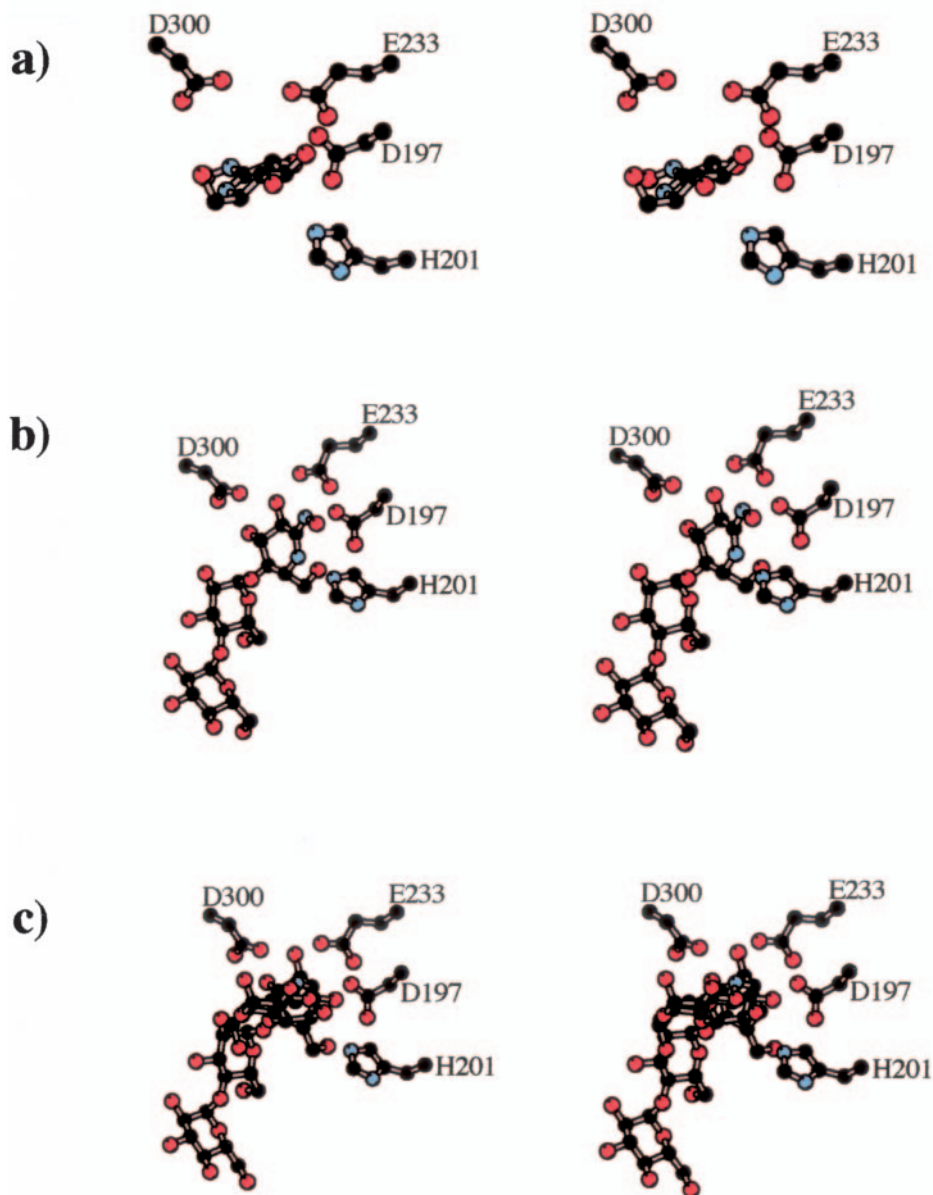


FIG. 8. Stereo drawings illustrating the bound conformations of the inhibitors GHIL (a), GHIL/G3F product (b), and acarbose (c) in the active site of HPA. Only selected active site residues are shown for clarity.

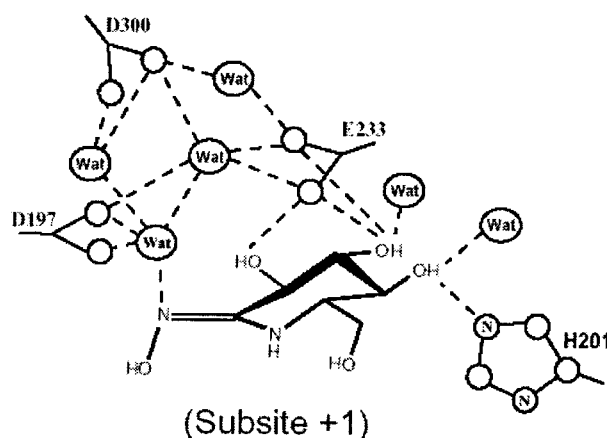
seen in the GHIL/HPA structure, these interactions would not be possible. Furthermore, comparison of the side chain position of Glu<sup>233</sup> in the G2-GHIL structure, with its position in the acarbose structure, indicates that it has rotated to accommodate this interaction with the oxime group. It has been suggested that the structurally similar gluconolactone is not a good inhibitor of  $\alpha$ -glucosidases because the lactone carbonyl group is not properly positioned for such interactions (29, 39). Similarly, the hydroximinolactone was also found to be a disappointing inhibitor, presumably for much the same reason (29). Indeed, it has been argued that the increased basicity of the exocyclic nitrogen conferred on it by the endocyclic nitrogen atom should strengthen the interaction between the oxime oxygen and catalytic acid/base residue sufficiently so that geometric penalties would be overcome. The present structural study indeed points toward exactly such a conformational adjustment in the case of the binding of GHIL to the  $-1$  subsite.

Another interaction is that between the catalytic nucleophile, Asp<sup>197</sup>, and the exocyclic nitrogen, where the Asp<sup>197</sup> is positioned perpendicular to the plane of the oxime with OD1

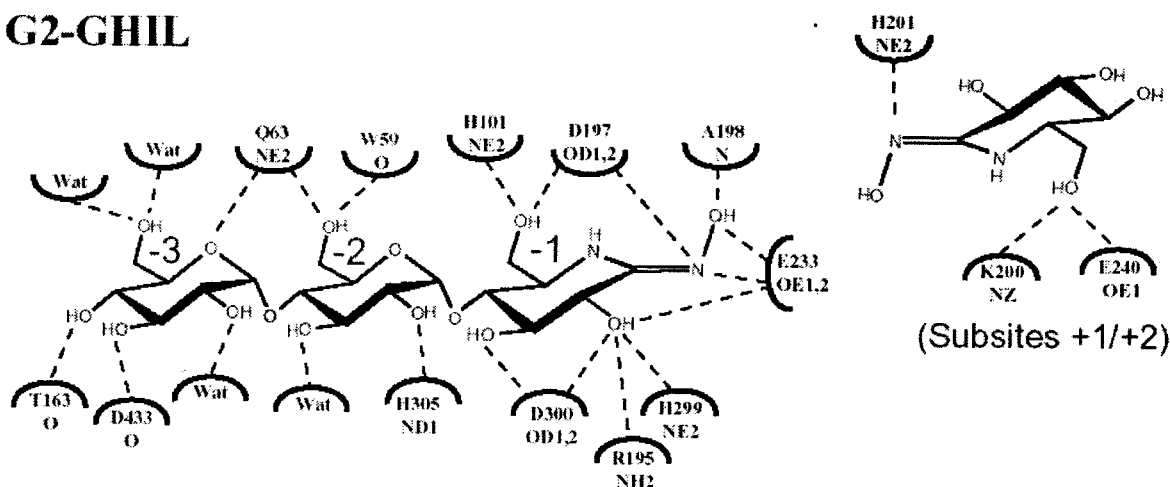
located 2.94 Å away from the exocyclic nitrogen. Surprisingly, OD2 of Asp<sup>197</sup> does not interact with the endocyclic nitrogen, as might have been expected on the basis of the interaction of the nucleophile with the glycosyl-enzyme intermediate in CGTase (9). Rather, it interacts with the 6-hydroxyl group, an interaction that is also present in the HPA-acarbose complex where no endocyclic heteroatom is present. Interactions of the 2- and 3-hydroxyl groups of the GHIL moiety with HPA are also very similar to those in the HPA-acarbose structure.

**Conclusions**—Although HPA is an important pharmaceutical target for controlling blood glucose levels, very few reports have been published on the development of novel inhibitors of this enzyme, in large part because of the difficulties encountered in the synthesis of oligosaccharide-based inhibitors. By taking advantage of the intrinsic ability of HPA to catalyze transglycosylation reactions, it is possible to elongate monosaccharide analogues *in situ* by preincubating the compound with an activated substrate (G3F). The formation of such elongated and more potent inhibitors from poorly

## a) GHIL



## b) G2-GHIL



## c) Acarbose

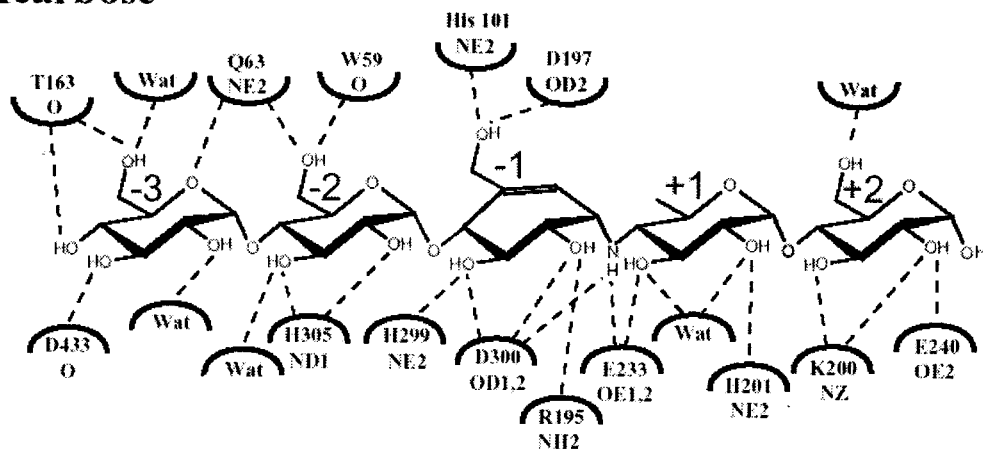


FIG. 9. Schematic diagrams illustrating the hydrogen bonding interactions ( $\leq 3.5$  Å) formed in the active site of HPA by GHIL (a), G2-GHIL formed on incubation with GHIL and G3F (b), and acarbose (c). The subsites of HPA occupied by each bound moiety are indicated, and interacting amino acids are designated with their one-letter codes.

binding monosaccharide analogues can be readily detected by assays with a slow substrate before and after preincubation with G3F. The specific structure of the elongated species and its interactions with the enzyme can be determined crystal-

lographically after incubating crystals with the monosaccharide analogue and G3F. This assay is easily adaptable to a 96-well plate format and is useful for the identification of potential elongated HPA inhibitors.

*Acknowledgments*—We thank Professor Vasella for the initial sample of GHIL and GelTex Inc. for the generous gift of CNP-G3.

## REFERENCES

1. Henrissat, B. (1991) *Biochem. J.* **280**, 309–316
2. Henrissat, B., and Bairoch, A. (1993) *Biochem. J.* **293**, 781–788
3. Henrissat, B., Callebaut, I., Fabrega, S., Lehn, P., Mornon, J. P., and Davies, G. (1995) *Proc. Natl. Acad. Sci. U. S. A.* **92**, 7090–7094
4. Aghajari, N., Feller, G., Gerday, C., and Haser, R. (1998) *Protein Sci.* **7**, 564–572
5. Brayer, G. D., Luo, Y., and Withers, S. G. (1995) *Protein Sci.* **4**, 1730–1742
6. Brzozowski, A. M., and Davies, G. J. (1997) *Biochemistry* **36**, 10837–10845
7. Machius, M., Wiegand, G., and Huber, R. (1995) *J. Mol. Biol.* **246**, 545–559
8. Kadziola, A., Abe, J., Svensson, B., and Haser, R. (1994) *J. Mol. Biol.* **239**, 104–121
9. Uitdehaag, J. C., Mosi, R., Kalk, K. H., van der Veen, B. A., Dijkhuizen, L., Withers, S. G., and Dijkstra, B. W. (1999) *Nat. Struct. Biol.* **6**, 432–436
10. Ramasubbu, N., Paloth, V., Luo, Y. G., Brayer, G. D., and Levine, M. J. (1996) *Acta Crystallogr. Sect. D Biol. Crystallogr.* **52**, 435–446
11. McCarter, J. D., and Withers, S. G. (1996) *J. Biol. Chem.* **271**, 6889–6894
12. Rydberg, E. H., Li, C., Maurus, R., Overall, C. M., Brayer, G. D., and Withers, S. G. (2002) *Biochemistry* **41**, 4492–4502
13. Tao, B. Y., Reilly, P. J., and Robyt, J. F. (1989) *Biochim. Biophys. Acta* **995**, 214–220
14. Sinnott, M. L. (1990) *Chem. Rev.* **90**, 1171–1202
15. Rye, C. S., and Withers, S. G. (2000) *Curr. Opin. Chem. Biol.* **4**, 573–580
16. Zechel, D. L., and Withers, S. G. (2000) *Acc. Chem. Res.* **33**, 11–18
17. Jenkins, D. J., Taylor, R. H., Goff, D. V., Fielden, H., Misiewicz, J. J., Sarson, D. L., Bloom, S. R., and Alberti, K. G. (1981) *Diabetes* **30**, 951–954
18. Meyer, B. H., Muller, F. O., Kruger, J. B., Clur, B. K., and Grigoleit, H. G. (1984) *S. Afr. Med. J.* **66**, 222–223
19. Taylor, R. H., Jenkins, D. J., Barker, H. M., Fielden, H., Goff, D. V., Misiewicz, J. J., Lee, D. A., Allen, H. B., MacDonald, G., and Wallrabe, H. (1982) *Diabetes Care* **5**, 92–96
20. Bailey, C. J. (1998) *Chem. Ind.* 53–57
21. Mosi, R., Sham, H., Uitdehaag, J. C. M., Ruiterkamp, R., Dijkstra, B. W., and Withers, S. G. (1998) *Biochemistry* **37**, 17192–17198
22. Brayer, G. D., Sidhu, G., Maurus, R., Rydberg, E. H., Braun, C., Wang, Y. L., Nguyen, N. T., Overall, C. M., and Withers, S. G. (2000) *Biochemistry* **39**, 4778–4791
23. Qian, M. X., Haser, R., Buisson, G., Duee, E., and Payan, F. (1994) *Biochemistry* **33**, 6284–6294
24. Brzozowski, A. M., Lawson, D. M., Turkenburg, J. P., Bisgaard-Frantzen, H., Svendsen, A., Borchert, T. V., Dauter, Z., Wilson, K. S., and Davies, G. J. (2000) *Biochemistry* **39**, 9099–9107
25. Takada, M., Ogawa, K., Saito, S., Murata, T., and Usui, T. (1998) *J. Biochem. (Tokyo)* **123**, 508–515
26. Takada, M., Ogawa, K., Murata, T., and Usui, T. (1999) *J. Carbohydr. Chem.* **18**, 149–163
27. Uchida, R., Nasu, A., Tokutake, S., Kasai, K., Tobe, K., and Yamaji, N. (1999) *Chem. Pharm. Bull.* **47**, 187–193
28. Yoon, S. H., and Robyt, J. F. (2003) *Carbohydr. Res.* **338**, 1969–1980
29. Hoos, R., Vasella, A., Rupitz, K., and Withers, S. G. (1997) *Carbohydr. Res.* **298**, 291–298
30. Rydberg, E. H., Sidhu, G., Vo, H. C., Hewitt, J., Cote, H. C., Wang, Y., Numao, S., MacGillivray, R. T., Overall, C. M., Brayer, G. D., and Withers, S. G. (1999) *Protein Sci.* **8**, 635–643
31. Hayashi, M., Hashimoto, S., and Noyori, R. (1984) *Chem. Lett.*, 1747–1750
32. Fleet, G. W. J., Carpenter, N. M., Petursson, S., and Ramsden, N. G. (1990) *Tetrahedron Lett.* **31**, 409–412
33. Hoos, R., Naughton, A. B., Thiel, W., Vasella, A., Weber, W., Rupitz, K., and Withers, S. G. (1993) *Helv. Chim. Acta* **76**, 2666–2686
34. Leatherbarrow, R. J. (1998) *Grafit*, 4.0.21 Ed., Erithacus Software Ltd., Staines, UK
35. Otwinowski, Z., and Minor, W. (1997) *Method Enzymol.* **276**, 307–326
36. Brunger, A. T., Adams, P. D., Clore, G. M., DeLano, W. L., Gros, P., Grosse-Kunstleve, R. W., Jiang, J. S., Kuszewski, J., Nilges, M., Pannu, N. S., Read, R. J., Rice, L. M., Simonson, T., and Warren, G. L. (1998) *Acta Crystallogr.* **54**, 905–921
37. Jones, T. A., Zhou, J.-Y., Cowan, S. W., and Kjeldgaard, M. (1991) *Acta Crystallogr. Sect. A* **47**, 110–119
38. Notenboom, V., Williams, S. J., Hoos, R., Withers, S. G., and Rose, D. R. (2000) *Biochemistry* **39**, 11553–11563
39. Heightman, T. D., and Vasella, A. T. (1999) *Angew. Chem. Int. Ed. Engl.* **38**, 750–770